RESEARCH ARTICLE

Design and Experiments of a Machine Vision-Based Directional Arrangement Device for Packaged Vegetables

Zhien Zhang[1,2], **Weiwei Chen**[1,2], **Huichan Huang**[3] **and Shenyuan Dai**[1,2,*]

[1] Wenzhou Academy of Agricultural Sciences, Wenzhou 325006, China
[2] Wenzhou Key Laboratory of AI Agents for Agriculture, Wenzhou 325006, China
[3] Yueqing Bureau of Agriculture and Rural Affairs, Wenzhou 325600, China

Abstract

Plant factories, as agricultural production systems characterized by high yield, efficient resource utilization, and advanced mechanization, have attracted increasing global attention. Packaging finished vegetables is a critical pre-shipment operation in plant-factory production, and its automation and intelligent control remain urgent research needs. In vegetable-packaging line, an orientation-adjustment mechanism is required to correct the posture of packaged vegetables so that the boxing mechanism can place them neatly in turnover boxes. The operation of this mechanism depends on accurate identification of vegetable orientation. In this study, packaged vegetables produced in a plant factory were selected as the research object. Their postures on a conveyor belt were simulated, and images were acquired for orientation recognition. Multiple image features and classifiers were compared, and suitable texture features and classifiers were selected to identify the orientation of packaged vegetables. A translating-oscillating compound cam mechanism was designed according to the motion requirements for flipping packaged vegetables. The design process included determination of the follower motion law, generation of the cam profile curve, establishment of the cam model, and optimization of the structural parameters through a human-computer interaction framework. A prototype was then fabricated and assembled, and tests were conducted to verify the accuracy of the visual recognition system and the feasibility of the steering mechanism. The results showed that the GA-SVM classifier achieved a maximum accuracy of 97.90% with the fused HOG and GLCM features. The average accuracy of the recognition model was 95.27%, and the success rate of the steering mechanism was 94.67%. Both the recognition and steering performances were satisfactory. The proposed orientation-identification method and turning mechanism for packaged vegetables in plant factories were successfully implemented, providing a technical basis for unmanned plant-factory production lines.

Keywords: machine vision, plant factory, mechanism design, head-tail orientation, prototype testbed.

Submitted: 16 May 2026
Accepted: 22 June 2026
Published: 29 June 2026

Vol. 2, **No.** 2, 2026.
10.62762/DIA.2026.219926

***Corresponding author:**
✉ Shenyuan Dai
daishenyuan@wzvcst.edu.cn

Citation
Zhang, Z., Chen, W., Huang, H., & Dai, S. (2026). Design and Experiments of a Machine Vision-Based Directional Arrangement Device for Packaged Vegetables. *Digital Intelligence in Agriculture*, 2(2), 103–113.

1 Introduction

Plant factories are recognized for their efficient resource use, high sustainability, and advanced automation, and are increasingly regarded as an important direction for future agriculture [1]. Their growing global acceptance is reflected in rising consumer interest and positive attitudes toward plant-factory products across multiple regions [2]. Among the operations involved in plant-factory production, vegetable packaging remains one of the most critical yet least automated processes. Proper packaging is essential not only for operational efficiency but also for maintaining product quality during post-harvest handling and distribution [3]. Because the head and tail ends of vegetables are visually distinguishable, their orientation must be identified and corrected to achieve uniform alignment before packaging.

Machine vision has been widely applied in agricultural production, including harvesting, sorting, and quality inspection [4, 5]. Accordingly, orientation and posture estimation have attracted considerable research interest. Kok and Chen [6] applied deep learning to estimate apple orientation under orchard occlusion, addressing the lack of distinctive features and enabling adaptive grasping by harvesting robots. Wang et al. [7] used YOLOv5 to determine apple placement orientation based on stem detection. Lin et al. [8] segmented strawberry fruit and calyx regions based on color differences and identified their respective orientations to guide calyx removal. Beyond harvesting, orientation detection has also been applied to pollination using PSTL_Orient for pistil measurement [9], to navel-orange posture adjustment for citrus detection [10], and to YOLOv5s-based orientation recognition for Panax notoginseng root transplanting [11, 12].

Neat packaging requires products to be properly oriented before they enter the carton. In this context, flexible clamping and conveying mechanisms have been developed to handle leafy vegetables in an orderly manner during the harvesting and post-harvest transport stages that precede packaging [13]. Several mechanical orientation strategies have been reported for agricultural and aquatic products. For fish, Wan et al. [14] combined machine vision with a vibrating conveyor and roller squeezing to achieve head-tail and belly-back adjustment. For garlic cloves, which are smaller and less uniform, Hou et al. [15] designed a regulating device and a multi-feature recognition algorithm to determine clove orientation for precision planting, while Chen et al. [16] proposed a machine vision-based mechanical orientation mechanism that adjusts garlic posture using head and tail image features.

In summary, many studies have investigated crop orientation recognition by combining various features with different classification methods. However, limited attention has been given to orientation recognition for packaged vegetables in plant factories. Similarly, steering and conveying mechanisms for packaged-vegetable transportation in such facilities remain underexplored. To address the directional conveyance of packaged vegetables in plant factories, this study proposes a Support Vector Machine (SVM)-based orientation-recognition method. By integrating this method with a translating-oscillating compound cam steering mechanism, a complete cam-based steering system for packaged vegetables was developed.

2 Materials and Methods

2.1 Vision-Based Mechanism Design for Packaged Vegetables

In this study, a machine learning-based method was used to identify the head-tail orientation of packaged vegetables, and a translating-oscillating compound cam steering mechanism was designed to perform head-tail reversal. By integrating real-time orientation recognition, the steering mechanism selectively adjusts the posture of packaged vegetables. The overall workflow is illustrated in Figure 1.

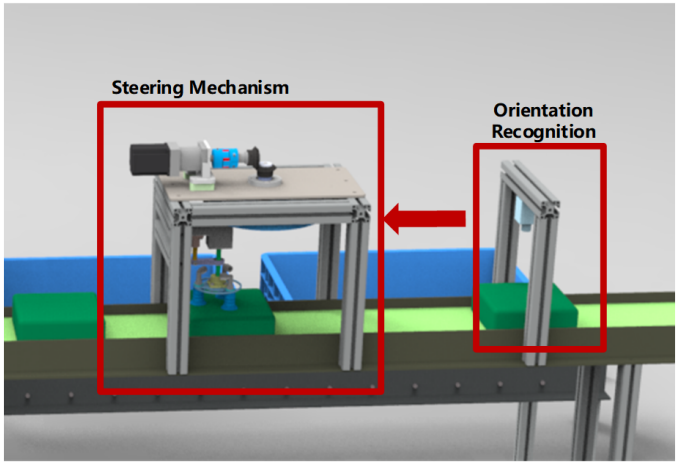

Figure 1. Operation flow chart of the proposed mechanism.

Considering the agronomic requirements, the key components of the translating-oscillating compound cam steering mechanism were optimally designed, and the overall structure is shown in Figure 2. The

compound cam is driven by a stepper motor to execute posture adjustment, which consists of grasping and turning actions. The outer surface of the compound cam contains a cylindrical cam profile for a translating follower. This profile drives a translating roller, causing the vertical shaft to reciprocate vertically and thereby executing the grasping motion of the end-effector disk. The bottom of the compound cam contains a planar cam profile for an oscillating follower. This profile drives an oscillating roller, causing the oscillating lever to swing and thereby achieving the turning motion of the end-effector disk. The vertical shaft and oscillating lever operate alternately to complete the posture-adjustment process.

2.2 Machine Learning-Based Orientation Recognition for Packaged Vegetables

Packaged lettuce was used as the experimental material for image acquisition. Otsu's method and morphological operations were used for background segmentation and preprocessing of the packaged-vegetable images. Three types of image features were extracted and subsequently fused. A comparative evaluation was then conducted to select an appropriate feature-fusion strategy and classifier.

2.2.1 Image Preprocessing and Feature Extraction

The packaged lettuce samples were placed horizontally on the conveyor belt, and images were acquired from a distance of 35 cm directly above the samples. A total of 500 images with a resolution of 1024 × 1280 pixels were collected. To improve processing efficiency, the images were compressed to 256 × 256 pixels. The images were then converted from RGB to HSV color space, and the H channel was selected for binarization using Otsu's method. A morphological closing operation, consisting of dilation followed by erosion, was subsequently applied to improve the quality of the binary images. After background segmentation and preprocessing, image texture features were extracted for orientation recognition of the packaged vegetables. The selected features included the Histogram of Oriented Gradients (HOG), Local Binary Pattern (LBP), and Gray-Level Co-occurrence Matrix (GLCM). To avoid the adverse effect of feature redundancy on recognition accuracy, this study did not directly combine all three features. This approach is consistent with findings from SVM-based agricultural image recognition, where selective feature combination has been shown to outperform exhaustive feature merging in discriminating visually similar plant structures [17]. Instead, different feature combinations

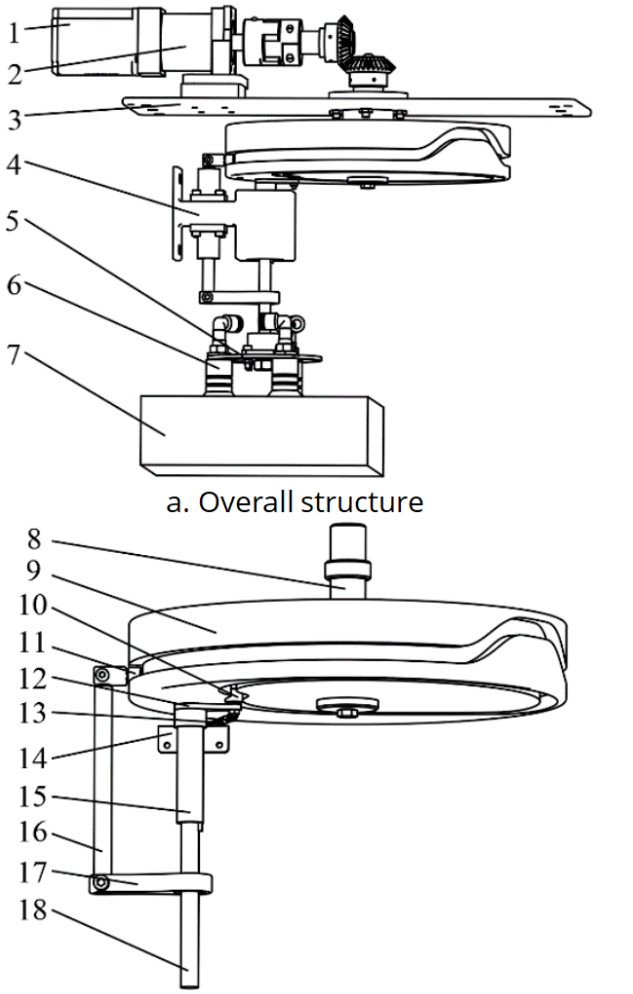

Figure 2. Overall structure of the translating-oscillating compound cam steering mechanism. 1. Stepper motor; 2. Reducer; 3. Fixed upper plate; 4. Fixed frame; 5. End-effector disk; 6. Suction cups; 7. Packaged vegetables; 8. Rotating spindle; 9. Translating-oscillating compound cam; 10. Oscillating roller; 11. Translating roller; 12. Oscillating lever; 13. Spring; 14. Spring fixing frame; 15. Sleeve; 16. Movable shaft; 17. Connecting plate; 18. Shift shaft.

were constructed and compared to determine the most suitable feature representation for packaged-vegetable orientation recognition.

2.2.2 Machine Learning-Based Orientation Recognition Model for Packaged Vegetables

A Support Vector Machine (SVM) was used for binary sample classification. SVMs have been widely adopted in agricultural image recognition tasks, demonstrating strong generalization performance across diverse crop sensing and detection scenarios [18]. Furthermore, the choice of feature dimensionality and representation strategy significantly affects classifier performance,

Table 1. Average evaluation metrics of different classifiers under different feature-fusion strategies.

Classifier	Evaluation Metrics	Feature-Fusion Strategies						
		HOG	LBP	GLCM	HOG +LBP	HOG +GLCM	LBP +GLCM	HOG+LBP +GLCM
GA-SVM	Acc	96.26	93.16	94.27	96.75	97.90	95.82	97.59
	P	96.22	89.89	95.10	96.46	97.72	93.81	97.43
	R	97.18	97.28	96.61	96.77	98.06	96.89	97.80
	F1-score	96.14	93.26	95.07	96.58	97.87	95.68	97.58
KNN	Acc	93.14	91.91	92.87	95.30	96.07	92.70	96.74
	P	94.61	92.32	93.92	96.03	96.58	95.84	97.82
	R	86.36	91.22	89.71	90.65	92.14	89.34	96.65
	F1-score	92.51	91.52	92.47	93.04	94.79	92.27	97.16
RF	Acc	95.89	93.02	94.13	96.39	95.73	94.37	95.86
	P	95.89	93.45	95.42	96.27	95.91	96.11	95.84
	R	95.87	92.15	92.89	96.32	96.34	92.43	96.36
	F1-score	95.83	93.59	93.95	96.18	95.70	94.07	95.69

as high-dimensional feature spaces can introduce redundancy and degrade accuracy [19]. The SVM used a radial basis function (RBF) kernel, and its classification performance depends strongly on the kernel parameter γ and the penalty parameter C. Because classification accuracy is highly sensitive to these two parameters, a genetic algorithm (GA) was adopted for parameter optimization. With classification accuracy used as the fitness function, the GA was configured with a population size of 50, a crossover probability of 0.7, and a mutation probability of 0.05. After 100 generations, the optimized classifier, GA-SVM, was obtained. The dataset, comprising positive and negative samples, was randomly divided into a training set (80%) and a testing set (20%). The HOG, LBP, and GLCM features were combined to create seven feature combinations. To evaluate classifier performance, K-Nearest Neighbors (KNN), Random Forest (RF), and the optimized GA-SVM were tested on datasets corresponding to the seven feature combinations. Each model was trained and tested independently 10 times. Accuracy, precision, recall, and F1-score were recorded for each run, and the average values of these four metrics over the 10 runs were used as the final evaluation metrics. These metrics are defined as follows:

$$\text{ACC (accuracy)} = \frac{TP + TN}{TP + FP + TN + FN} \quad (1)$$

$$P \text{ (precision)} = \frac{TP}{TP + FP} \quad (2)$$

$$R \text{ (recall)} = \frac{TP}{TP + FN} \quad (3)$$

$$\text{F1-score} = \frac{2 \times P \times R}{P + R} \quad (4)$$

where TP, FP, TN, and FN denote true positives, false positives, true negatives, and false negatives, respectively. The F1-score balances the precision and recall of the classification model.

Because the three feature types yielded seven possible combinations, the three classifiers were trained on each feature combination to evaluate the performance advantage of the GA-SVM classifier relative to KNN and RF. Accuracy, precision, recall, and F1-score were recorded for each combination. As shown in Table 1, the GA-SVM classifier achieved the highest accuracy, 97.90%, when the fused HOG and GLCM features were used. By comparison, the highest average accuracies of the KNN and RF classifiers were 96.74% and 96.39%, respectively. The GA-SVM classifier also consistently outperformed the alternative models in the other evaluation metrics. Therefore, GA-SVM was selected as the final classifier for packaged-vegetable orientation recognition, and the fused HOG and GLCM features were adopted as the optimal texture-feature representation.

2.3 Design of Key Components of the Translating-Oscillating Compound Cam Steering Mechanism

A translating-oscillating compound cam steering mechanism for packaged vegetables was designed in this study. The motion laws were formulated according to agronomic requirements, the profile curves of the key components were designed, and

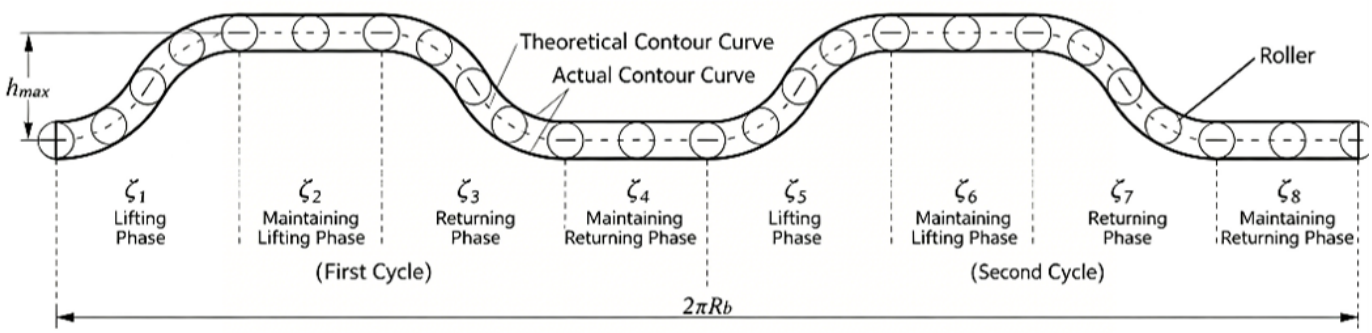

Figure 3. Cylindrical cam spread profile working section.

the corresponding three-dimensional models were established.

2.3.1 *Structure and Working Principle of the Steering Mechanism for Packaged Vegetables*

The translating-oscillating compound cam steering mechanism consists of a translating-oscillating compound cam, a translating rod, an oscillating lever, a suction disk, springs, and other components. The steering mechanism is mounted above the conveyor belt, and a motor drives the compound cam to rotate. When the lateral cylindrical cam is in the return-dwell phase, the bottom oscillating cam is in the non-dwell phase, enabling the packaged vegetables to be turned.

For a single steering operation, the lateral cylindrical cam sequentially passes through the return, return-dwell, rise, and rise-dwell phases. Simultaneously, the bottom oscillating cam passes through the near-dwell phase, the outstroke/return-stroke phase, and the far-dwell phase. Specifically, the return-dwell phase corresponds to the outstroke/return-stroke phase. As a result, the suction disk moves vertically downward, rotates 180° horizontally, and then returns to its initial position, completing one full turning cycle for the packaged vegetable. Because the oscillating cam must include both an outstroke and a return stroke, the lateral cylindrical cam is designed to complete one cycle every 180° to avoid idle rotation, whereas the oscillating cam completes one cycle every 360°.

2.3.2 *Design of the Cylindrical Cam and Determination of Its Motion Law*

According to the agronomic requirements, the lift of the cylindrical cam was set to 20 mm. The distribution of the working segments of the cam profile is illustrated in Figure 3. To achieve smooth posture adjustment of the packaged vegetables, the return-dwell phase was extended to $2\pi/3$. The rise phase, rise-dwell phase, and return phase were set to $5\pi/36$, $\pi/18$, and $5\pi/36$, respectively.

A quintic polynomial motion law was adopted to design the cam profile curve, reduce impact, and ensure smooth motion [20]. The displacement of the follower is expressed as follows:

$$h = \begin{cases} h_{\max}\left[10\left(\frac{\theta}{\zeta_1}\right)^3 - 15\left(\frac{\theta}{\zeta_1}\right)^4 + 6\left(\frac{\theta}{\zeta_1}\right)^5\right], & 0 \le \theta \le \frac{5\pi}{36} \\ h_{\max}, & \frac{5\pi}{36} \le \theta \le \frac{7\pi}{36} \\ h_{\max} - h_{\max}\left[10\left(\frac{\theta-\frac{7\pi}{36}}{\zeta_3}\right)^3 - 15\left(\frac{\theta-\frac{7\pi}{36}}{\zeta_3}\right)^4 + 6\left(\frac{\theta-\frac{7\pi}{36}}{\zeta_3}\right)^5\right], & \frac{7\pi}{36} \le \theta \le \frac{\pi}{3} \\ 0, & \frac{\pi}{3} \le \theta \le \pi \\ h_{\max}\left[10\left(\frac{\theta-\pi}{\zeta_5}\right)^3 - 15\left(\frac{\theta-\pi}{\zeta_5}\right)^4 + 6\left(\frac{\theta-\pi}{\zeta_5}\right)^5\right], & \pi \le \theta \le \frac{41\pi}{36} \\ h_{\max}, & \frac{41\pi}{36} \le \theta \le \frac{43\pi}{36} \\ h_{\max} - h_{\max}\left[10\left(\frac{\theta-\frac{43\pi}{36}}{\zeta_7}\right)^3 - 15\left(\frac{\theta-\frac{43\pi}{36}}{\zeta_7}\right)^4 + 6\left(\frac{\theta-\frac{43\pi}{36}}{\zeta_7}\right)^5\right], & \frac{43\pi}{36} \le \theta \le \frac{4\pi}{3} \\ 0, & \frac{4\pi}{3} \le \theta \le 2\pi \end{cases} \tag{5}$$

where h is the lift height, $h_{\max}$ is the maximum lift height, and θ is the rotation angle of the cylindrical cam.

By unfolding the base-cylinder surface of the cylindrical cam, the developed planar profile curve is obtained as follows:

$$\begin{cases} x_B = R_b\theta \\ y_B = h \end{cases} \tag{6}$$

where R_b is the base-circle radius, x_B is the horizontal coordinate of the developed theoretical profile curve,

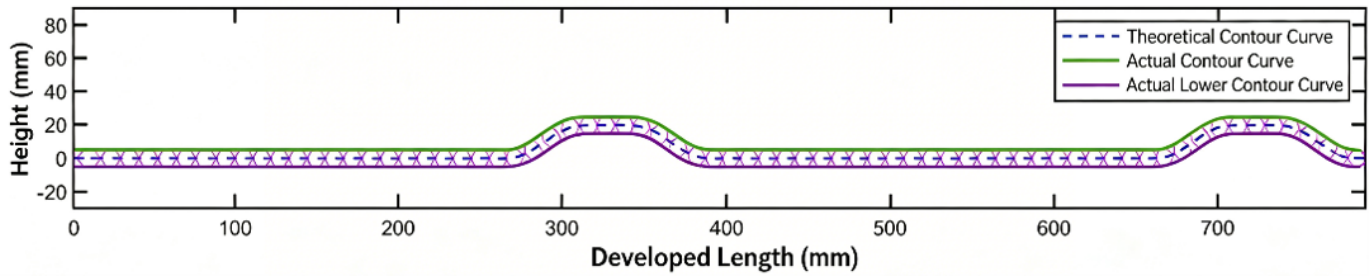

Figure 4. Cylindrical roller straight moving follower planar cam profile curve.

and y_B is the vertical coordinate of the developed theoretical profile curve.

After the roller radius R was set to 5 mm and the base-circle radius of the cylindrical cam was set to 125 mm, the theoretical and actual cam profile curves were obtained, as shown in Figure 4.

2.3.3 *Determination of Follower Motion Laws and Basic Parameters of the Planar Grooved Cam*

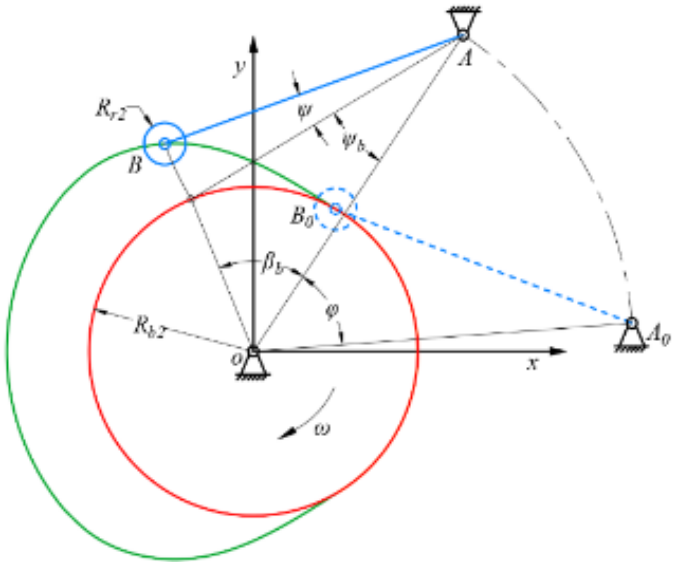

Figure 5. Schematic diagram of the oscillating cam mechanism.

The outstroke angle, far-dwell angle, return-stroke angle, and near-dwell angle of the planar grooved cam were $2\pi/3$, $\pi/3$, $2\pi/3$, and $\pi/3$, respectively. The outstroke/return-stroke phase corresponds to the return-dwell phase of the cylindrical cam, whereas the near/far dwell phase corresponds to the sum of the rise, rise-dwell, and return phases of the cylindrical cam. A schematic of the cam mechanism is shown in Figure 5, where β_b and ψ_b are the angles of the oscillating lever at its initial position; φ is the cam rotation angle; ψ is the rotation angle of the oscillating lever; L_{AB} is the length of the oscillating lever; L_{OA} is the distance between the cam rotation center O and the lever rotation center A; R_{b2} is the base-circle radius of the cam; and R_{f2} is the roller radius.

Using a fifth-degree polynomial motion law, the follower displacement is given by:

$$\psi = \begin{cases} \psi_{\max}\left[10\left(\frac{\varphi}{\delta_1}\right)^3 - 15\left(\frac{\varphi}{\delta_1}\right)^4 \right. \\ \left. +6\left(\frac{\varphi}{\delta_1}\right)^5\right], & 0 \le \varphi \le \frac{2\pi}{3} \\ \psi_{\max}, & \frac{2\pi}{3} \le \varphi \le \pi \\ \psi_{\max} - \psi_{\max}\left[10\left(\frac{\varphi-\pi}{\delta_3}\right)^3 \right. \\ \left. -15\left(\frac{\varphi-\pi}{\delta_3}\right)^4 + 6\left(\frac{\varphi-\pi}{\delta_3}\right)^5\right], & \pi \le \varphi \le \frac{5\pi}{3} \\ 0, & \frac{5\pi}{3} \le \varphi \le 2\pi \end{cases} \tag{7}$$

where $\psi_{\max}$ denotes the maximum angular displacement.

The theoretical cam profile curve is obtained using the inversion method, as follows:

$$\begin{cases} \theta_b = \arctan\left[\frac{L_{OA}\sin(\varphi-\beta_b)-L_{AB}\sin[\varphi-(\beta_b+\psi_b+\psi)]}{L_{OA}\cos(\varphi-\beta_b)-L_{AB}\cos[\varphi-(\beta_b+\psi_b+\psi)]}\right] \\ \rho_b = L_{OA}\cos(\varphi-\beta_b-\theta_b) \\ \qquad -L_{AB}\cos[\varphi-(\beta_b+\psi_b+\psi)-\theta_b] \end{cases} \tag{8}$$

where

$$\begin{cases} \beta_b = \arccos\left[\frac{R_{b2}^2+L_{OA}^2-L_{AB}^2}{2R_{b2}L_{OA}}\right] \\ \psi_b = \arccos\left[\frac{L_{OA}^2+L_{AB}^2-R_{b2}^2}{2L_{OA}L_{AB}}\right] \end{cases} \tag{9}$$

After setting the roller radius R_f to 5 mm, the actual profile curve of the grooved cam is expressed as

follows:

$$\begin{cases} \theta_k = & \arctan\left[\dfrac{\rho_b \sin\theta_b + \lambda R_{r2}\sin\left[\varphi-\left(\frac{\pi}{2}+\beta_b+\psi_b+\psi\right)-\alpha\right]}{\rho_b \cos\theta_b + \lambda R_{r2}\cos\left[\varphi-\left(\frac{\pi}{2}+\beta_b+\psi_b+\psi\right)-\alpha\right]}\right] \\ \rho_k = & \rho_b\cos(\theta_b-\theta_k) \\ & +\lambda R_{r2}\cos\left[\varphi-\left(\frac{\pi}{2}+\beta_b+\psi_b+\psi\right)-\alpha-\theta_k\right] \end{cases} \tag{10}$$

The cam profile curve was then solved using the above equations.

Table 2. Oscillating follower plane groove cam mechanism parameters.

Mechanism parameter	Numerical value
Base radius	65 mm
Distance between centers	90 mm
Pendulum length	25 mm
Roller radius	5 mm

The parameters of the grooved cam profile are listed in Table 2, and the profile curve is shown in Figure 6.

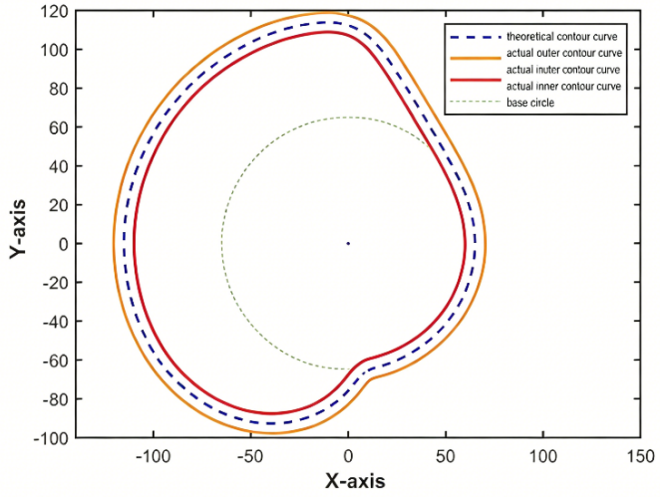

Figure 6. Profile curve of the planar grooved cam with an oscillating follower.

3 Results and Discussion

To verify the applicability of the proposed recognition model and the translating-oscillating compound cam steering mechanism for packaged vegetables, an experimental testbed was constructed and evaluated.

3.1 Prototype Manufacturing and Assembly

The experimental testbed is shown in Figure 7. The translating-oscillating compound cam was fabricated by resin 3D printing. The remaining components were procured as standard parts, and the prototype was then assembled.

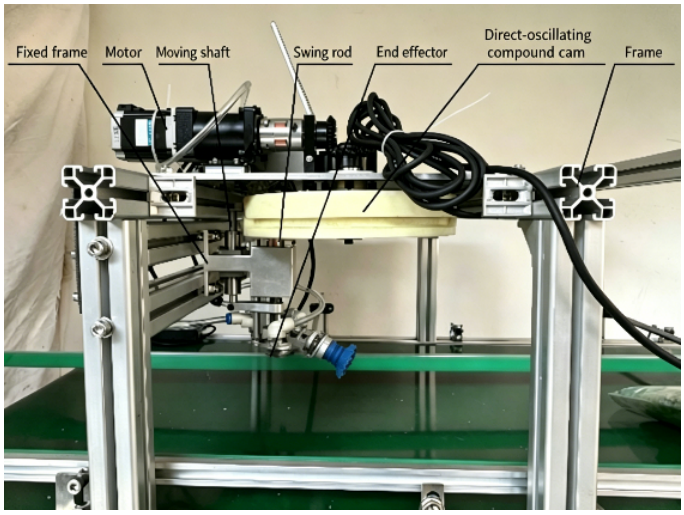

Figure 7. Translating-oscillating compound cam steering mechanism.

The assembled steering mechanism was mounted above the packaged-vegetable conveyor belt using an aluminum-profile frame, and an industrial camera was installed approximately 30 cm upstream. This layout provided sufficient processing time for image acquisition, recognition, and classification before the packaged vegetables reached the execution area. Finally, the recognition results were transmitted to the microcontroller, which commanded the steering mechanism to execute the corresponding actions, thereby achieving the directional arrangement of the packaged vegetables.

3.2 Experimental Evaluation Criteria

Packaged vegetables were used as the test samples, and the following evaluation metrics were established: orientation recognition accuracy R_S was used to measure the performance of the recognition algorithm, and steering success rate R_F was used to evaluate the operational reliability of the steering mechanism. In addition, the operating speed of the steering mechanism was set to 60 packs/min to verify the overall system performance under continuous working conditions.

$$R_S = \left(1 - \frac{H_C}{H_Z}\right) \times 100\% \tag{11}$$

$$R_F = \left(1 - \frac{H_F}{H_Z}\right) \times 100\% \tag{12}$$

where H_Z is the total number of packaged vegetables, H_C is the number of incorrectly recognized packaged vegetables, and H_F is the number of packaged vegetables that failed to undergo the required adjustment.

a. Head-first recognition results

b. Tail-forward recognition result

Figure 8. Recognition results for the head-tail orientation of packaged vegetables.

3.3 Experimental Procedure and Results Analysis

To further verify the accuracy, the multi-feature fusion framework of Wang et al. [21], originally proposed for agricultural image classification, was adapted as a baseline by applying its 91-dimensional color, shape, and texture feature extraction pipeline to the orientation recognition task. Ten images were randomly selected as test samples, and the orientation recognition accuracy was used as the evaluation metric. As shown in Table 3, the high-dimensional features introduced redundancy and degraded recognition performance, leading to a lower average accuracy compared with the proposed method. This confirms the effectiveness of the GA-SVM based method for head-tail orientation recognition of packaged vegetables; some results are illustrated in Figure 8.

Table 3. Performance comparison of orientation recognition for packaged vegetables.

Samples	Wang's	This study
1	93.00%	93.33%
2	91.67%	96.67%
3	96.67%	95.00%
4	94.67%	96.67%
5	93.67%	95.00%
6	91.33%	95.33%
7	92.33%	94.33%
8	93.67%	95.67%
9	95.00%	94.33%
10	94.33%	96.33%

The steering mechanism operates according to the orientation-identification results and arranges the packaged vegetables in the required pattern. The adjustment process for a packaged vegetable is shown in Figure 9.

The suction disk picked up the packaged vegetables with reasonable accuracy, the head-tail reversal was successfully achieved, and the steering mechanism completed the prescribed motion. However, because the packaged vegetables varied in size, larger packages occasionally collided with the mechanism and showed slight damage, although this occurred at a low frequency. The recognition accuracy and steering success rate are summarized in Table 4.

As shown in Table 4, the steering mechanism achieved an average success rate of 94.67%, with a minimum of 91.67%. Both the recognition accuracy and steering success rate were high and operationally stable, satisfying the engineering requirements.

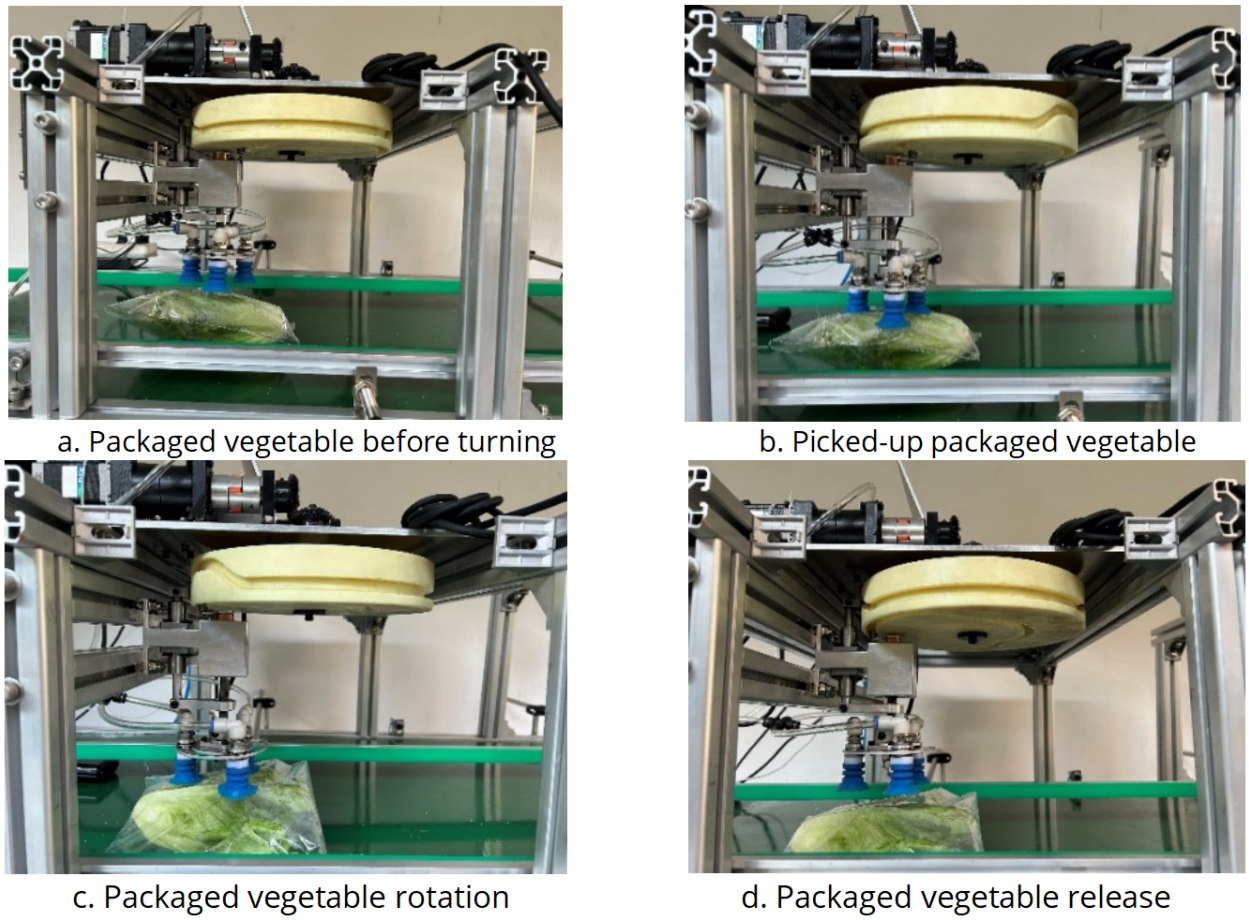

Figure 9. Flipping process of packaged vegetables.

Table 4. Experimental results for steering performance.

Samples	Steering success rate
1	95.00%
2	93.33%
3	98.33%
4	95.00%
5	91.67%
Average test result	94.67%

4 Conclusions

An SVM-based orientation-recognition method was developed to identify the head-tail orientation of packaged vegetables. Background segmentation was conducted using Otsu's method combined with morphological operations, and HOG, LBP, and GLCM texture features were extracted and fused. Among the RF, KNN, and GA-SVM classifiers, GA-SVM delivered the best performance, particularly under the HOG + GLCM feature-fusion strategy, yielding high recognition accuracy.

A translating-oscillating compound cam steering mechanism was developed to achieve the ordered arrangement of packaged vegetables through coordinated vertical and rotational motions. The prototype was fabricated and experimentally evaluated. The proposed posture-adjustment system achieved an average orientation recognition accuracy of 95.27%, and the steering mechanism achieved an average steering success rate of 94.67%, confirming that the system meets the engineering requirements for packaged-vegetable orientation adjustment.

Data Availability Statement

Data will be made available on request.

Funding

This work was supported by the Wenzhou Basic Scientific Research Project under Grant NC20250006 and the Industrial Upgrading Project of the Longwan Modern Agricultural Industry Research Institute under Grant 2025LWYJY09.

Conflicts of Interest

The authors declare no conflicts of interest.

AI Use Statement

The authors declare that no generative AI was used in the preparation of this manuscript.

Ethical Approval and Consent to Participate

Not applicable.

References

[1] Tian, Z., Ma, W., Yang, Q., & Duan, F. (2022). Application status and challenges of machine vision in plant factory—A review. *Information Processing in Agriculture, 9*(2), 195-211. [CrossRef]

[2] Ares, G., Ha, B., & Jaeger, S. R. (2021). Consumer attitudes to vertical farming (indoor plant factory with artificial lighting) in China, Singapore, UK, and USA: A multi-method study. *Food Research International, 150*, 110811. [CrossRef]

[3] Giannakourou, M. C., & Tsironi, T. N. (2021). Application of processing and packaging hurdles for fresh-cut fruits and vegetables preservation. *Foods, 10*(4), 830. [CrossRef]

[4] Wang, T., Chen, B., Zhang, Z., Li, H., & Zhang, M. (2022). Applications of machine vision in agricultural robot navigation: A review. *Computers and Electronics in Agriculture, 198*, 107085. [CrossRef]

[5] Chen, Y. R., Chao, K., & Kim, M. S. (2002). Machine vision technology for agricultural applications. *Computers and electronics in Agriculture, 36*(2-3), 173-191. [CrossRef]

[6] Kok, E., & Chen, C. (2024). Occluded apples orientation estimator based on deep learning model for robotic harvesting. *Computers and Electronics in Agriculture, 219*, 108781. [CrossRef]

[7] Wang, Z., Jin, L., Wang, S., & Xu, H. (2022). Apple stem/calyx real-time recognition using YOLO-v5 algorithm for fruit automatic loading system. *Postharvest Biology and Technology, 185*, 111808. [CrossRef]

[8] Lin, J., Holmes, M., Vinson, R., Ge, C., Pogoda, F. C., Mahon, L., ... & Tao, Y. (2017). Design and testing of an automated high-throughput computer vision guided waterjet knife strawberry calyx removal machine. *Journal of Food Engineering, 211*, 30-38. [CrossRef]

[9] Yang, M., Lyu, H., Zhao, Y., Sun, Y., Pan, H., Sun, Q., ... & Yang, H. (2023). Delivery of pollen to forsythia flower pistils autonomously and precisely using a robot arm. *Computers and Electronics in Agriculture, 214*, 108274. [CrossRef]

[10] Hao, Y., Wang, Q., & Zhang, S. (2021). Online accurate detection of soluble solids content in navel orange assisted by automatic orientation correction device. *Infrared Physics & Technology, 118*, 103871. [CrossRef]

[11] Lai, Q., Wang, Y., Tan, Y., & Sun, W. (2024). Design and experiment of Panax notoginseng root orientation transplanting device based on YOLOv5s. *Frontiers in Plant Science, 15*, 1325420. [CrossRef]

[12] Zhou, J., Zhang, P., Wei, M., Liu, W., Shi, J., Tan, Y., & Hu, J. (2026). Deep Learning-Based Recognition of Arch-Back Direction in Bare-Root Strawberry Seedlings for Mechanized Transplanting. *Agriculture, 16*(6), 657. [CrossRef]

[13] Jin, Y., Wang, J., Chen, J., Song, Z., Zhang, R., & Zhou, R. (2024). Design and experiment for flexible clamping and conveying device for green leafy vegetable orderly harvester. *Agriculture, 14*(6), 967. [CrossRef]

[14] WAN, P., HUANG, Y., WANG, R., LI, M., XIAO, C., & WU, W. (2023). Design and experiments of the machine vision-based body orientation arrangement convey device for the Scomber japonicus. *Transactions of the Chinese Society of Agricultural Engineering, 39*(14), 271-282. [CrossRef]

[15] Hou, J. L., Tian, L., Li, T. H., Niu, Z. R., & Li, Y. H. (2020). Design and experiment of test bench for garlic bulbil adjustment and seeding based on bilateral image identification. *Transactions of the CSAE, 36*(1), 50-58. [CrossRef]

[16] Chen, J., Yu, C., Yao, K., Zhou, Y., & Zhou, B. (2022). Design and experiment of a garlic orientation and orderly conveying device based on machine vision. *Agriculture, 12*(8), 1077. [CrossRef]

[17] Zhang, L., Zhang, Z., Wu, C., & Sun, L. (2022). Segmentation algorithm for overlap recognition of seedling lettuce and weeds based on SVM and image blocking. *Computers and Electronics in Agriculture, 201*, 107284. [CrossRef]

[18] Taha, M. F., Mao, H., Zhang, Z., Elmasry, G., Awad, M. A., Abdalla, A., ... & Elsherbiny, O. (2025). Emerging technologies for precision crop management towards agriculture 5.0: A comprehensive overview. *Agriculture, 15*(6), 582. [CrossRef]

[19] Howley, T., Madden, M. G., O'Connell, M. L., & Ryder, A. G. (2005, December). The effect of principal component analysis on machine learning accuracy with high dimensional spectral data. In International Conference on Innovative Techniques and Applications of Artificial Intelligence (pp. 209-222). London: Springer London. [CrossRef]

[20] Pozo-Palacios, J., Fulbright, N. J., Voth, J. A., & Van de Ven, J. D. (2023). Comparison of forward and inverse cam generation methods for the design of cam-linkage mechanisms. *Mechanism and Machine Theory, 190*, 105465. [CrossRef]

[21] Wang, Y., Zhang, X., Ma, G., Du, X., Shaheen, N., & Mao, H. (2021). Recognition of weeds at asparagus fields using multi-feature fusion and backpropagation neural network. *International Journal of Agricultural and Biological Engineering, 14*(4), 190-198. [CrossRef]

Zhien Zhang is a Research Intern at Wenzhou Academy of Agricultural Sciences, Wenzhou 325006,China. He holds a Master's degree in Mechanical Engineering. His research interests include mechanical structure design and smart agriculture. (Email: zhangzhien@wzvcst.edu.cn)

Huichan Huang serves as Director of Yueqing Agriculture and Rural Education & Training Center under the Yueqing Bureau of Agriculture and Rural Affairs. Her research interests include rural revitalization and smart agriculture. (Email: 41307984@qq.com)

Weiwei Chen is a Teaching Assistant at Wenzhou Academy of Agricultural Sciences, Wenzhou 325006, China. He holds a Master's degree in Agricultural Engineering and Information Technology. His research interests include image processing and smart agriculture. (Email: chenweiwei@wzvcst.edu.cn)

Shenyuan Dai is an Assistant Researcher at the Wenzhou Academy of Agricultural Sciences, Wenzhou 325006, China, He holds a Ph.D in Mechanical Engineering. His research interests include mechanisms & robotics and smart agriculture. (Email: daishenyuan@wzvcst.edu.cn)